Astron. Astrophys. 342, 337–352 (1999)

ASTRONOMY AND ASTROPHYSICS

Weak lensing and cosmology

Marco Lombardi and Giuseppe Bertin

Scuola Normale Superiore, Piazza dei Cavalieri 7, I-56126 Pisa, Italy

Received 17 June 1998 / Accepted 12 November 1998

Abstract. Recently, it has been shown that it is possible to reconstruct the projected mass distribution of a cluster from weak lensing provided that both the geometry of the universe and the probability distribution of galaxy redshifts are known; actually, when additional photometric data are taken to be available, the galaxy redshift distribution could be determined jointly with the cluster mass from the weak lensing analysis. In this paper we develop, in the spirit of a "thought experiment," a method to constrain the geometry of the universe from weak lensing, provided that the redshifts of the source galaxies are measured. The quantitative limits and merits of the method are discussed analytically and with a set of simulations, in relation to point estimation, interval estimation, and test of hypotheses for homogeneous Friedmann-Lemaître models. The constraints turn out to be significant when a few thousand source galaxies are used.

Key words: galaxies: clusters: general – galaxies: distances and redshifts – cosmology: observations – cosmology: dark matter – cosmology: gravitational lensing

1. Introduction

It has long been recognized (see Tyson et al. 1984) that the gravitational field of a cluster acts on the images of distant galaxies by changing their orientation so that their major axes tend to become perpendicular to the direction of the center of the cluster. In turn (see Kaiser & Squires 1993) the mean ellipticity of the galaxy images can be used to measure the shear of the lens, a quantity related to the two-dimensional mass distribution (projected along the line of sight). By now a number of reconstruction techniques have been proposed and tested (see, e.g., Kaiser et al. 1995; Seitz & Schneider 1996; Hoekstra et al. 1998).

In the reconstruction process, information on the ratio of the distances from the observer to the source galaxies and from the lens to the galaxies is used. In practice, in the limit where the galaxies are much farther than the lens, the reconstruction process becomes independent of the distance of the source galaxies (Schneider & Seitz 1995, Seitz & Schneider 1995). This, of course, is very useful, as usually the redshifts of the sources are not available. If this limit cannot be taken (as it happens if the cluster itself has a relatively high redshift, e.g., $z_{\rm d} \gtrsim 0.5$), then one has to take into account the different redshifts of the background galaxies. The result of the gravitational lensing *does depend* on the geometry of the universe.

Seitz & Schneider (1997) have shown that it is possible to reconstruct the mass distribution of the lens provided that both the probability distribution of galaxy redshifts and the geometry of the universe are known (e.g., the values of Ω and Ω_Λ in the standard Friedmann-Lemaître cosmology). If other data (in particular, the angular sizes and luminosities of the source galaxies) are taken to be available, then the problem of the joint determination of the galaxy redshift distribution and of the lens mass density, for an assumed geometry of the universe, can be solved using the so called "lens parallax method" (Bartelmann & Narayan 1995). This latter method is based on the decrease of the surface brightness of galaxies and on the corresponding increase of the lens strength with redshift. A third possibility, of determining the properties of the lens and the geometrical characteristics of the universe from an assumed knowledge of the distances to the source galaxies, is not natural because of the prohibitive demands posed by the measurement of a large number of redshifts. However, this last option is actually most natural *in principle*, given the fact that redshifts are the quantities that can be best measured *directly*.

In recent years the technique to obtain photometric redshifts (Baum 1962) has been greatly improved and tested. A large number of photometric redshifts of very faint sources ($m_B > 25$) can be obtained without additional telescope time (with respect to imaging). For the Hubble Deep Field more than one thousand photometric redshifts have been estimated (Lanzetta et al. 1996). Moreover, the technique can be rather accurate (provided that a good set of filters is used). For example, in a first test on a sample of 27 galaxies in the Hubble Deep Field, by comparison with the spectroscopic redshifts now available, more than 68% of the photometric redshifts have errors $|\Delta z| < 0.1$, and all redshifts have errors $|\Delta z| < 0.3$ (Hogg et al. 1998). This suggests that in a not far future we might use photometric redshift information for galaxies lensed by a cluster.

Send offprint requests to: M. Lombardi
Correspondence to: lombardi@sns.it

In this paper we show how we can determine both the lens mass distribution and the geometry of the universe if the redshifts of the source galaxies are known. The method outlined here could be used, in a Friedmann-Lemaître universe, to get information on the density parameter Ω and on the cosmological constant parameter Ω_Λ, or could be used to test different cosmologies. At this stage the study proposed here may be seen as a "thought experiment" because of the very high number of redshifts that are found to be required in order to constrain the geometry significantly. We will show below that the galaxies that one should observe can hardly be found behind a single cluster at the magnitudes currently attainable. However, it is possible to combine data from different clusters. Combining the study of 5–10 clusters would lead to statistically meaningful constraints. With such a device, the application of the present method might even become feasible in a not too far future. Surprisingly, simulations show that the method applied to observations considered to be realistic for current plans of the Next Generation Space Telescope (NGST) should provide significant constraints on the cosmological parameters even if based on a single cluster.

The paper is organized as follows. In Sect. 2 we recall the main lensing equations generalized to sources at different distances and introduce the "cosmological weight," a quantity that gives the strength of the lens scaled to the relevant distances involved. The reconstruction of the cluster mass distribution and of the cosmological weight is described in Sect. 3. Sect. 4 addresses the issue of the invariance properties associated with the reconstruction analysis. Sect. 5 introduces the determination of the cosmological parameters by recognizing the limits on the measurement of the cosmological weight. The results of a wide set of simulations are described in detail in Sect. 6. Sect. 7 addresses the problem of the actual feasibility of a measurement based on the procedure outlined in the paper. Finally, in Sect. 8, we summarize the main results obtained. Four appendices contain detailed discussions and derivations of some important results.

2. Distance dependent lensing relations

This section is aimed at defining the basic mathematical framework and mostly follows the article by Seitz & Schneider (1997). Let us consider a lens at redshift z_d with two-dimensional projected mass distribution $\Sigma(\boldsymbol{\theta})$, where $\boldsymbol{\theta}$ is a two-dimensional vector representing a direction on the sky (the region of interest on the sky is very small and can be considered flat). For a source at redshift z we define the critical density $\Sigma_\mathrm{c}(z)$ as

$$\Sigma_\mathrm{c}(z) = \begin{cases} \infty & \text{for } z \le z_\mathrm{d} \ , \\ \dfrac{c^2 D(z)}{4\pi G D(z_\mathrm{d}) D(z_\mathrm{d}, z)} & \text{otherwise} \ . \end{cases} \tag{1}$$

Here $D(z)$ and $D(z_\mathrm{d}, z)$ are, respectively, the angular diameter-distance from the observer to an object at redshift z, and from the lens to the same object. The quantities $D(z_\mathrm{d})$, $D(z)$, and $D(z_\mathrm{d}, z)$ replace the Euclidean distances, respectively D_od, D_os, and D_ds, used in Paper I (Lombardi & Bertin 1998a).

It is useful to define a redshift independent critical density as

$$\Sigma_\mathrm{c}^\infty = \lim_{z\to\infty} \Sigma_\mathrm{c}(z) \ , \tag{2}$$

related to the redshift dependent critical density through a "cosmological weight" function

$$w(z) = \frac{\Sigma_\mathrm{c}^\infty}{\Sigma_\mathrm{c}(z)} \propto \frac{D(z_\mathrm{d}, z)}{D(z)} \ . \tag{3}$$

In principle, the above relations could be the starting point also for investigations based on non-standard cosmological models, using the constraints on the cosmological weight $w(z)$ provided by the gravitational lensing analysis to be described below. In practice, for the rest of the paper we will focus on the standard Friedmann-Lemaître cosmology, where the angular diameter-distance $D(z)$ can be written as (Peebles 1993; see also Kayser et al. 1997)

$$D(z) = D(0, z) \ , \tag{4}$$

$$D(z_\mathrm{d}, z) = \frac{c}{H_0 (1+z) \sqrt{\Omega_R}} \sinh\left[\sqrt{\Omega_R} \int_{z_\mathrm{d}}^{z} \frac{\mathrm{d}z'}{E(z')} \right] , \tag{5}$$

where

$$E(z') = \sqrt{\Omega (1+z')^3 + \Omega_R (1+z')^2 + \Omega_\Lambda} \ , \tag{6}$$

and, we recall, $\Omega + \Omega_\Lambda + \Omega_R = 1$. The hyperbolic sine in Eq. (5) is characteristic of an open universe ($\Omega_R > 0$).

In general, $w(z) \to 1$ for $z \to \infty$. As we will see shortly, the lensing equations depend on the geometry via the cosmological weight, and thus this is the function that can be determined from lensing observations. The function depends in a complicated manner on the two cosmological parameters Ω and Ω_Λ. For an Einstein-de Sitter universe ($\Omega = 1$, $\Omega_\Lambda = 0$, so that $\Omega_R = 0$) one has, for $z > z_\mathrm{d}$,

$$\frac{H_0 D(z_\mathrm{d}, z)}{c} = \frac{2}{1+z} \left(\frac{1}{\sqrt{1+z_\mathrm{d}}} - \frac{1}{\sqrt{1+z}} \right) \ , \tag{7}$$

$$w(z) = \frac{\sqrt{1+z} - \sqrt{1+z_\mathrm{d}}}{\sqrt{1+z} - 1} \ . \tag{8}$$

Some examples of weight functions for a lens at redshift $z_\mathrm{d} = 0.8$ are given in Fig. 1. It should be noted that the cosmological weights for "reasonable" universes lie very close to each other. This of course makes the determination of the cosmological parameters from the measurement of the cosmological weight a difficult task.

For sources at redshift z, we define the Jacobian matrix of the ray-tracing function as (see Eq. (3) of Paper I)

$$\begin{aligned} A(\boldsymbol{\theta}, z) \ &= \ \left(\frac{\partial \boldsymbol{\theta}^\mathrm{s}}{\partial \boldsymbol{\theta}} \right) \\ &= \ \begin{pmatrix} 1 - w(z)(\kappa - \gamma_1) & w(z)\gamma_2 \\ w(z)\gamma_2 & 1 - w(z)(\kappa + \gamma_1) \end{pmatrix} \ . \end{aligned} \tag{9}$$

Here $\kappa = \kappa(\boldsymbol{\theta}) = \Sigma(\boldsymbol{\theta})/\Sigma_\mathrm{c}^\infty$ is the lens density in units of the redshift independent critical density defined in Eq. (2), while

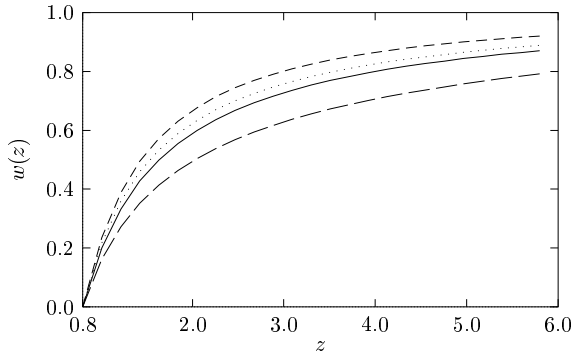

Fig. 1. The weight function for a lens at $z_{\rm d} = 0.8$ in four different universes. From the top to the bottom: $\Omega = 0.3$, $\Omega_\Lambda = 0$ (dashed); $\Omega = 0.3$, $\Omega_\Lambda = 0.7$ (dotted); $\Omega = 1$, $\Omega_\Lambda = 0$ (solid); $\Omega = 1$, $\Omega_\Lambda = 1$ (long dashed).

$\gamma = \gamma(\boldsymbol{\theta})$ is the complex shear. Then the redshift dependent amplification $\mu(\boldsymbol{\theta}, z)$ is given by

$$\begin{aligned} \frac{1}{\mu(\boldsymbol{\theta}, z)} &= \left|\det A(\boldsymbol{\theta}, z)\right| \\ &= \left[1 - w(z)\kappa(\boldsymbol{\theta})\right]^2 - \left|w(z)\gamma(\boldsymbol{\theta})\right|^2 . \end{aligned} \tag{10}$$

This expression gives the magnification produced by the lens on a source located at redshift z. If this quantity can be measured (for example by using galaxy counts), the mass density of the lens can be constrained strongly, and an otherwise present invariance property (see Sect. 4) can be broken.

For a galaxy at redshift z seen at position $\boldsymbol{\theta}$ a complex quantity ϵ is defined in terms of the galaxy quadrupole moment Q_{ij} (see Schneider & Seitz 1995 for a detailed discussion):

$$\epsilon = \frac{Q_{11} - Q_{22} + 2\mathrm{i}Q_{12}}{Q_{11} + Q_{22} + 2\sqrt{Q_{11}Q_{22} - Q_{12}^2}} . \tag{11}$$

At variance with Paper I and Paper II (Lombardi & Bertin 1998b), it is convenient to measure the ellipticity using this quantity instead of χ (see Eq. (7) of Paper I), because of the simpler transformation properties of ϵ (see Eq. (14) below). In fact, as shown by Seitz & Schneider (1997), the observed ellipticity is related to the source ellipticity through the relation (the superscript stands for "source")

$$\epsilon = \begin{cases} \dfrac{\epsilon^{\rm s} - g(\boldsymbol{\theta}, z)}{1 - g^*(\boldsymbol{\theta}, z)\epsilon^{\rm s}} & \text{for } \left|g(\boldsymbol{\theta}, z)\right| \le 1 , \\ \dfrac{1 - g(\boldsymbol{\theta}, z)\epsilon^{\rm s*}}{\epsilon^{\rm s*} - g^*(\boldsymbol{\theta}, z)} & \text{otherwise} , \end{cases} \tag{12}$$

where the reduced shear $g(\boldsymbol{\theta}, z)$ is defined as

$$g(\boldsymbol{\theta}, z) = \frac{w(z)\gamma(\boldsymbol{\theta})}{1 - w(z)\kappa(\boldsymbol{\theta})} . \tag{13}$$

From the observation of a large number of galaxies near $\boldsymbol{\theta}$, with redshifts close to z, we can thus determine the reduced shear $g(\boldsymbol{\theta}, z)$. In fact, it can be shown that the expected mean value of the observed ellipticities is given by

$$\langle\epsilon\rangle(\boldsymbol{\theta}, z) = \begin{cases} -g(\boldsymbol{\theta}, z) & \text{if } \left|g(\boldsymbol{\theta}, z)\right| < 1 , \\ -\dfrac{1}{g^*(\boldsymbol{\theta}, z)} & \text{otherwise} , \end{cases} \tag{14}$$

under the isotropy hypothesis $\langle\epsilon^{\rm s}\rangle = 0$ for the source galaxy distribution. This expression depends on the redshift of the galaxies used. Therefore, if we measure the mean value of the ellipticities for galaxies at different redshifts, we can obtain information on the cosmological weight function $w(z)$. Once the cosmological weight function $w(z)$ has been determined, the cluster mass reconstruction can be performed using an iterative procedure on Eq. (13), seeded by $\kappa = 0$, and some kernel analysis (see Paper II). As shown by Seitz & Schneider (1997), this can be carried out even if one does not have the redshift of each galaxy, provided one knows the galaxy probability distribution in z.

In the rest of the paper we assume that the ellipticity dispersion of the source galaxies is independent of redshift (see also App. C).

3. Joint determination of the shear and of the cosmological weight

Let us now address the goal of this paper, the joint determination of the lens mass and of the geometry of the universe. In the following, for simplicity, we will consider a cluster subcritical for all z, i.e. a cluster that cannot produce multiple images, characterized by $\left|g(\boldsymbol{\theta}, z)\right| < 1$ for all $\boldsymbol{\theta}$ and all z (from Eq. (10), by recalling that subcritical lenses are also characterized by $\det A > 0$, it can be shown that this happens when $\kappa(\boldsymbol{\theta}) + \left|\gamma(\boldsymbol{\theta})\right| < 1$ for every $\boldsymbol{\theta}$). General clusters could be treated basically in the same way, but with considerably heavier notation. Let the positions $\boldsymbol{\theta}^{(n)}$, the observed ellipticities $\epsilon^{(n)}$, and the redshifts $z^{(n)}$ of N source galaxies ($n = 1, \ldots, N$) be known, together with the redshift $z_{\rm d}$ of the cluster.

In the following we will use subscript 0 for *true* quantities. For example, κ_0 will be the true dimensionless surface density of the lens, and $w_0(z)$ the true cosmological weight (given by Eq. (3)). For the complex quantities γ and g we will use the notation γ_{0i} and g_{0i} to denote the i-th component of the true value. Following the notation used in statistics, we will use hats for *measured* quantities ("estimators"). Thus $\hat{\kappa}(\boldsymbol{\theta})$ will be the measured mass density, and $\hat{w}(z)$ the measured cosmological weight.

In order to describe the reconstruction process, we start by considering the weak lensing limit, and then we generalize the results obtained.

3.1. Weak lensing limit

The weak lensing limit is characterized by $\left|\gamma_0(\boldsymbol{\theta})\right|, \kappa_0(\boldsymbol{\theta}) \ll 1$, so that the reduced shear $g_0(\boldsymbol{\theta}, z)$ can be identified with the product $w_0(z)\gamma_0(\boldsymbol{\theta})$. In this limit Eqs. (12) and (14) become

$$\epsilon = \epsilon^{\rm s} - \gamma_0(\boldsymbol{\theta})w_0(z) \tag{15}$$

and

$$\langle\epsilon\rangle(\boldsymbol{\theta}, z) = -\gamma_0(\boldsymbol{\theta})w_0(z) . \tag{16}$$

These relations allow us to estimate, from a set of measurements $\left\{\epsilon^{(n)}\right\}$, one of the two quantities, either the shear or the cosmological weight function, provided the other is known. The basic

idea is to average the observed ellipticities of galaxies close to each other either in $\boldsymbol{\theta}$-space or in redshift, following the general theory of maximum likelihood methods to minimize errors (e.g., see Eadie et al., 1971).

If we take $w(z)$ to be known, we can introduce the *spatial* weight function $W(\boldsymbol{\theta},\boldsymbol{\theta}')$ with the property that $W(\boldsymbol{\theta},\boldsymbol{\theta}')$ is significantly different from zero only for $\|\boldsymbol{\theta}-\boldsymbol{\theta}'\|$ small (see Kaiser & Squires 1993; Paper II). Then, from Eq. (15), the shear $\gamma(\boldsymbol{\theta})$ can be estimated by

$$\hat{\gamma}(\boldsymbol{\theta}) = -\frac{\sum_{n=1}^{N} W\big(\boldsymbol{\theta},\boldsymbol{\theta}^{(n)}\big) w\big(z^{(n)}\big) \epsilon^{(n)}}{\sum_{n=1}^{N} W\big(\boldsymbol{\theta},\boldsymbol{\theta}^{(n)}\big) \big[w\big(z^{(n)}\big)\big]^2} \; . \tag{17}$$

Here, we recall, the cosmological weight function is taken to be known.

Similarly, if we take the shear $\gamma(\boldsymbol{\theta})$ to be available, we can introduce a *redshift* weight function $W_z(z,z')$, with the condition that $W_z(z,z')$ is significantly different from zero only for $|z-z'|$ small. Then the cosmological weight function $w(z)$ can be estimated by

$$\hat{w}(z) = -\frac{\sum_{n=1}^{N} W_z\big(z,z^{(n)}\big) \Re\big[\gamma\big(\boldsymbol{\theta}^{(n)}\big) \epsilon^{(n)*}\big]}{\sum_{n=1}^{N} W_z\big(z,z^{(n)}\big) \big|\gamma\big(\boldsymbol{\theta}^{(n)}\big)\big|^2} \; , \tag{18}$$

where $\Re$ and the asterisk denote real part and complex conjugate (we recall that ϵ and γ are complex quantities).

The two equations can be used to obtain by *iteration* the joint determination of the shear and of the cosmological weight function. We start with a guess for the weight function $w(z)$ (e.g., the expression known for the Einstein-de Sitter cosmology given in Eq. (8)), and calculate the shear using Eq. (17). Then we insert the estimated shear $\hat{\gamma}(\boldsymbol{\theta})$ in Eq. (18) and thus obtain a first estimate for $w(z)$. We then go back to Eq. (17) and obtain a new determination of $\hat{\gamma}(\boldsymbol{\theta})$, etc.

As a by-product of the analysis, by means of standard methods (Seitz & Schneider 1996; Paper II), we can also reconstruct, from the estimate $\hat{\gamma}(\boldsymbol{\theta})$, the dimensionless mass distribution $\kappa(\boldsymbol{\theta})$.

At the end of the iteration process, it can be shown that the procedure leads to the correct determination of $w(z)$, in the sense that

$$\langle\hat{w}\rangle(z) \simeq \frac{\sum_{n=1}^{N} W_z\big(z,z^{(n)}\big) w_0\big(z^{(n)}\big)}{\sum_{n=1}^{N} W_z\big(z,z^{(n)}\big)} \simeq w_0(z) \; . \tag{19}$$

Further discussion of Eqs. (17) and (18) is given in App. C.

3.2. General case

If the lens is not weak the solution of our problem is more complicated and requires nesting two different iteration processes. Let us start by assuming that the cosmological weight is known. A relation between $\gamma(\boldsymbol{\theta})$ and the observed ellipticities now involves the quantity $\kappa(\boldsymbol{\theta})$, as can be easily found from Eqs. (13) and (14):

$$\hat{\gamma}(\boldsymbol{\theta}) = -\frac{\displaystyle\sum_{n=1}^{N} W\big(\boldsymbol{\theta},\boldsymbol{\theta}^{(n)}\big) \left[\frac{w\big(z^{(n)}\big)}{1-w\big(z^{(n)}\big)\hat{\kappa}\big(\boldsymbol{\theta}^{(n)}\big)}\right] \epsilon^{(n)}}{\displaystyle\sum_{n=1}^{N} W\big(\boldsymbol{\theta},\boldsymbol{\theta}^{(n)}\big) \left[\frac{w\big(z^{(n)}\big)}{1-w\big(z^{(n)}\big)\hat{\kappa}\big(\boldsymbol{\theta}^{(n)}\big)}\right]^2} \; . \tag{20}$$

It is not difficult to recognize that this equation, which generalizes Eq. (17), leads to the optimal estimation of γ_0. We note that the combination of weights is again optimized with regard to the error on γ. It is clear that Eq. (20) can be used to obtain both the shear γ and the mass density κ, provided that we know the cosmological weight. To this purpose we can use an initial guess for $\hat{\kappa}(\boldsymbol{\theta})$ (e.g., $\hat{\kappa}(\boldsymbol{\theta}) = 0$) in Eq. (20), obtaining in this way a first estimation of $\gamma(\boldsymbol{\theta})$. From this we can obtain, using standard methods (see Kaiser 1995, Seitz & Schneider 1996, and Paper I and II for a discussion), the corresponding mass density, up to a constant. Then we can go back to Eq. (20) with the mass density and obtain a new determination of $\hat{\gamma}$, and so on. The method outlined here is similar to that described by Seitz & Schneider (1997), with the important difference that they cannot use the weights $w\big(z^{(n)}\big)$ in Eq. (20) since the galaxy redshifts are not taken to be known.

For given values of $\gamma(\boldsymbol{\theta})$ and $\kappa(\boldsymbol{\theta})$ we can estimate $w(z)$ in a manner similar to the weak lensing limit. In the general case Eq. (18) is replaced by

$$\begin{aligned}\hat{w}(z) = -\; & \left[\sum_{n=1}^{N} W_z\big(z,z^{(n)}\big)\big[1-w\big(z^{(n)}\big)\kappa\big(\boldsymbol{\theta}^{(n)}\big)\big]^{-1} \times \right. \\ & \left. \times \quad \Re\big[\gamma^*\big(\boldsymbol{\theta}^{(n)}\big)\epsilon^{(n)}\big]\right] \times \\ & \times \left[\sum_{n=1}^{N} W_z\big(z,z^{(n)}\big) \left|\frac{\gamma\big(\boldsymbol{\theta}^{(n)}\big)}{1-w\big(z^{(n)}\big)\kappa\big(\boldsymbol{\theta}^{(n)}\big)}\right|^2\right]^{-1}\end{aligned} \tag{21}$$

As in the weak lensing limit, the joint determination of γ and w is performed by an iterative process between Eq. (20) and Eq. (21). However, we stress once more that in this case Eq. (20) requires a separate iteration for the joint determination of γ and κ, to be performed between Eq. (20) and some kernel analysis for mass reconstruction (see Paper II).

The proof that Eq. (21) leads to an estimation of $w_0(z)$ would be similar to that for Eq. (18).

4. Invariance properties

So far, we have assumed that the shear map $\gamma(\boldsymbol{\theta})$, the mass distribution $\kappa(\boldsymbol{\theta})$, and the cosmological weight $w(z)$ can be determined uniquely. Unfortunately, two invariance properties affect the lensing equations and leave the reconstruction process ambiguous.

The first property is the well known "sheet-invariance" (Kaiser & Squires 1993; Schneider & Seitz 1995). In the weak lensing limit, this affects only the dimensionless mass density

$\kappa(\boldsymbol{\theta})$ and has a simple interpretation. If we add a homogeneous "sheet" to the mass density all equations remain unchanged.

The second invariance property, that we call "global scaling invariance," is a new feature associated with the process of the joint determination of the lens mass density and of the cosmological weight.

4.1. Weak lensing limit

In this limit the two invariance properties refer to the transformations (sheet)

$$\kappa(\boldsymbol{\theta}) \mapsto \kappa(\boldsymbol{\theta}) + C \ , \quad \gamma(\boldsymbol{\theta}) \mapsto \gamma(\boldsymbol{\theta}) \ , \quad w(z) \mapsto w(z) \ , \quad (22)$$

and (global scaling)

$$\kappa(\boldsymbol{\theta}) \mapsto k\kappa(\boldsymbol{\theta}) \ , \quad \gamma(\boldsymbol{\theta}) \mapsto k\gamma(\boldsymbol{\theta}) \ , \quad w(z) \mapsto \frac{w(z)}{k} \ . \quad (23)$$

We note that, in the weak lensing limit, the two invariance properties are *decoupled*, in the sense that the first involves only the dimensionless density and the second is met in the determination of the cosmological weight (see Sect. 3.1) even without considering the estimation of the dimensionless density.

4.2. General case

In the general case, the two invariance properties are *coupled*, because all three basic quantities κ, γ, and w have to be determined jointly. In particular, when the lens is not weak, a new undesired source of uncertainty in the determination of the cosmological weight is introduced by the sheet invariance itself.

The sheet invariance arises because of the differential relation between $\gamma(\boldsymbol{\theta})$ and $\kappa(\boldsymbol{\theta})$. Let us recall the method used to obtain the dimensionless density map $\kappa(\boldsymbol{\theta})$ from the shear $\gamma(\boldsymbol{\theta})$. First the vector field (Kaiser 1995)

$$\boldsymbol{u}(\boldsymbol{\theta}) = -\begin{pmatrix} \gamma_{1,1} + \gamma_{2,2} \\ \gamma_{2,1} - \gamma_{1,2} \end{pmatrix} \quad (24)$$

is calculated from the shear map. As shown by a simple calculation, this vector field is the gradient of the mass density, i.e. $\nabla\kappa(\boldsymbol{\theta}) = \boldsymbol{u}(\boldsymbol{\theta})$. Hence, from the shear γ, the density κ can be determined only up to a constant. This is the usual sheet invariance in the weak lensing limit, where the shear is the observed quantity.

In the general case one cannot measure $\gamma(\boldsymbol{\theta})$ directly because Eq. (20), used to obtain the shear, involves the dimensionless mass density. In addition, a simple generalization to a relation $\nabla\tilde{\kappa} = \tilde{u}$ (see Kaiser 1995 and Paper II) is not available because of the presence of the cosmological weight (see, however, Seitz & Schneider 1997 for an approximate relation). Thus an iterative process is needed. In the iteration, the arbitrary constant used to invert the vector field $\boldsymbol{u}$ into the density map κ and the cosmological weight act in a complicated manner, which is hard to describe analytically. If the lens is sub-critical and if the cosmological weight is left unchanged (i.e. if the outer iteration is not performed, see Sect. 3), the sheet invariance can be expressed by (see Appendix A)

$$\kappa \mapsto \frac{C\langle w\rangle_z}{\langle w^2\rangle_z} + (1-C)\kappa(\boldsymbol{\theta}) \ , \quad \gamma(\boldsymbol{\theta}) \mapsto (1-C)\gamma(\boldsymbol{\theta}) \ , \quad (25)$$

where $\langle\cdot\rangle_z$ is the average over the redshifts. A similar expression has been found by Seitz & Schneider (1997), by considering the sheet invariance in a different context (the lens reconstruction for a population of galaxies with known redshift distribution). Unfortunately, even under the above special conditions, if one introduces the transformation (25) in Eq. (21), the resulting measured cosmological weight $w(z)$ changes in a complicated manner. It can be shown that the related transformation for the cosmological weight cannot be reduced to a simple scaling $w(z) \mapsto \nu w(z)$.

The global scaling invariance property is a the same as that encountered in the weak lensing limit; but here we recall that the three quantities γ, w, and κ have to be determined jointly. In particular, if we consider the transformation

$$\kappa(\boldsymbol{\theta}) \mapsto k\kappa(\boldsymbol{\theta}) \ , \quad \gamma(\boldsymbol{\theta}) \mapsto k\gamma(\boldsymbol{\theta}) \ , \quad w(z) \mapsto \frac{w(z)}{k} \ , \quad (26)$$

all equations remain unchanged. We observe that a similar invariance property is met when one derives information on the geometry of the universe from the separation of multiple images produced by a strong lens.

4.3. General strategy

In conclusion, there are two invariance properties, sheet and global scaling invariance. In the general case, both invariance properties affect the determination of the cosmological weight $w(z)$: the global scaling acts as a simple scaling, while the sheet invariance acts in a different and a priori unknown manner. Therefore, to the extent that the impact of the sheet invariance remains out of control, any determination of the cosmological weight would be useless. This implies that when the lens is not weak we can choose between two possibilities. Either we discard the central part of the cluster, leaving only the parts where the lens is weak, or we must find a way to break the sheet invariance.

As discussed by Seitz & Schneider (1997), there are several possible ways to break the sheet invariance. A simple and useful method is based on the *magnification effect* (Broadhurst et al. 1995), i.e. on the observed (local or total) number of galaxies. In the case of a single redshift source population, a simple expression holds (see Appendix B) for the total projected mass associated with κ

$$M = \int \kappa(\boldsymbol{\theta})\,\mathrm{d}^2\theta = \frac{1}{2}\int \left[1 - \det A(\boldsymbol{\theta})\right]\mathrm{d}^2\theta \ . \quad (27)$$

This has a very simple interpretation. Suppose that galaxies are distributed on the source plane with constant number density ρ^{s}. Then, the observed number density $\rho(\boldsymbol{\theta})$ (number of galaxies per square arcsec) is given by

$$\rho(\boldsymbol{\theta}) = \rho^{\mathrm{s}}\left|\det A(\boldsymbol{\theta})\right| = \frac{\rho^{\mathrm{s}}}{\mu(\boldsymbol{\theta})} \ . \quad (28)$$

Inserted in Eq. (27) it gives

$$\hat{M} = \frac{1}{2\rho^{\mathrm{s}}} \int \left[\rho^{\mathrm{s}} - \rho(\boldsymbol{\theta}) \operatorname{sgn} A(\boldsymbol{\theta})\right] \mathrm{d}^2\theta = \frac{N_{\mathrm{exp}} - (N_{\mathrm{I}} + N_{\mathrm{III}} - N_{\mathrm{II}})}{2\rho^{\mathrm{s}}} \,. \tag{29}$$

In this expression $\operatorname{sgn} A(\boldsymbol{\theta}) = \operatorname{sgn}\big(\det A(\boldsymbol{\theta})\big)$ is the sign of the determinant of $A(\boldsymbol{\theta})$, N_i is the observed number of images of kind i (see Schneider et al. 1992 for the relevant classification of images), and N_{exp} the expected number of galaxies in an area equal to that used for the observations. (We note that the classification of an observed image is easy once the critical lines can be determined empirically.)

In view of the above discussion, in the following we will always consider either the weak lensing limit or the general case with the sheet mass degeneracy broken. Simulations show that, for the present problem, a (not too "strange") lens with $\kappa \lesssim 0.3$ everywhere can be considered to be weak, i.e. to meet the asymptotic requirements $\kappa, |\gamma| \ll 1$. The global scaling invariance, instead, will be addressed explicitly in the analysis, i.e. it will be considered present and not broken.

One might think that the global scaling invariance could be broken simply by the use of the asymptotic behaviour of $w(z)$ at $z \to \infty$, i.e. by setting the cosmological weight equal to unity at high redshifts. Unfortunately, the asymptotic regime is reached only slowly. Thus only galaxies at very high redshifts (say $z \gtrsim 10$) would be useful, which is practically beyond the limits of observations. Still, in the discussion of the simulations (see Sect. 6), we will show that the fact that the global scaling invariance, in contrast with the sheet invariance, can be reduced to a simple scaling, allows us to proceed to a meaningful determination of the cosmological parameters (once the sheet invariance is assumed to be broken). In fact, we will fit the *shape* of the measured cosmological weight with a set of cosmological weights (corresponding to different cosmological parameters), leaving unspecified the *scale* of the function.

5. Limits on the determination of the cosmological weight function

In principle, given a determination of the cosmological weight function $w(z)$ from the procedure outlined in Sect. 3, it is straightforward to derive information on the parameters Ω and Ω_Λ that characterize the assumed Friedmann-Lemaître cosmology. In particular, we may resort to a simple least squares or maximum likelihood method. Such a method is able to lead not only to "point estimations" of the cosmological parameters, but also to "interval estimations," based on the identification of the relevant "confidence level" regions (see Appendix D). In practice, difficulties arise because the determination of $w(z)$ will remain incomplete:

- The *scale* of the cosmological weight is expected to be *unknown*, because of the global scaling invariance described in Sect. 4.
- The measurement of $w(z)$ is going to be restricted to a *limited redshift interval* and we anticipate to be able to do so with only *limited redshift resolution*.
- The measurement of $w(z)$, resulting from the study of a finite number of source galaxies, is going to be affected by *statistical errors*.

Therefore, we now need to determine, for every cosmological model, both the expected *measured* cosmological weight $\langle w \rangle(z)$ and the related error (covariance matrix). As we described in Paper II, since we are dealing with *functions*, either of space $\kappa(\boldsymbol{\theta})$ or of redshift $w(z)$, the covariance matrix analysis has to be extended to the related two-point correlation functions. These calculations can be carried out either analytically (see Appendix C) or numerically, through Monte Carlo simulations. In any case, we may anticipate that while an error on the expected measured $\langle w \rangle(z)$ introduces a *bias* in the estimation of the cosmological parameters, an error on the (co)variance of the cosmological weight is only bound to increase the expected variance of the cosmological parameters thus determined, which is not critical for point estimations.

6. Simulations

6.1. Method

We refer to a cluster at redshift $z_{\mathrm{d}} = 0.8$. Different geometries of the universe set different values for the critical density $\Sigma_{\mathrm{c}}^{\infty}$. In particular, calling $h = H_0/(100\mathrm{km\ s^{-1}Mpc^{-1}})$ the reduced Hubble constant, the case $\Omega = 1$, $\Omega_\Lambda = 0$ has $\Sigma_{\mathrm{c}}^{\infty} = 5.49\, h\mathrm{kg\ m^{-2}}$, while the case $\Omega = 0.3$, $\Omega_\Lambda = 0.7$ has $\Sigma_{\mathrm{c}}^{\infty} = 3.99\, h\mathrm{kg\ m^{-2}}$. In the following we specify the cluster mass distribution directly in dimensionless form. For this we consider the sum of a diffuse component A (a truncated Hubble profile) and three compact objects B, C, D. The corresponding (projected) two-dimensional distributions are

$$\kappa = \begin{cases} K_0 \dfrac{\sqrt{1 - r^2/R^2}}{1 + r^2/r_0^2} & \text{for } r < R \,, \\ 0 & \text{otherwise} \,, \end{cases} \tag{30}$$

and

$$\kappa = \frac{K_0}{1/r_0 - 1/R} \left(\frac{1}{\sqrt{r_0^2 + r^2}} - \frac{1}{\sqrt{R^2 + r^2}} \right) \,. \tag{31}$$

Here r denotes the angular distance from the center of each object. For simplicity of notation, we use the same symbols K_0, r_0, R for three scales, taken to be different in each case (see Table 1). The dimensionless density $\kappa(\boldsymbol{\theta})$ is calculated on a grid of 50×50 points (corresponding to a field of $5' \times 5'$ on the sky). The cluster, shown in Fig. 2, has a mass (for $h = 0.5$, $\Omega = 1$, and $\Omega_\Lambda = 0$) within a 1 Mpc aperture diameter of about $2 \times 10^{15}\,\mathrm{M}_\odot$. From the lens equations we calculate the shear γ on the same grid. Within the Friedmann-Lemaître geometry, the weight function is calculated directly from Eqs. (3), (4), and (5). For the purpose, 25 equally spaced points in redshift from $z_{\mathrm{d}} = 0.8$ to $z_{\mathrm{d}} = 5.8$ are found to be sufficient.

Table 1. The parameters used for the four components of the cluster mass distribution. Component A is a Hubble profile, components B, C, and D represent compact objects ("dominant" galaxies).

Comp.	Center θ_1	Center θ_2	Inner scale r_0	Outer scale R	Density K_0
A	$0'\ 0''$	$0'\ 0''$	$1'\ 15''$	$4'\ 0''$	0.5
B	$0'\ 0''$	$+0'\ 30''$	$0'\ 9''$	$0'\ 30''$	0.2
C	$-1'\ 30''$	$-1'\ 0''$	$0'\ 15''$	$1'\ 0''$	0.3
D	$+1'\ 0''$	$-0'\ 30''$	$0'\ 9''$	$0'\ 30''$	0.1

The ellipticities of source galaxies are generated using a truncated Gaussian distribution

$$p\big(|\epsilon^{\rm s}|\big) = \frac{1}{\pi P^2\big[1-\exp(-1/P^2)\big]}\exp\Big(-|\epsilon^{\rm s}|^2/P^2\Big)\ , \qquad (32)$$

with $P = 0.15$. Note that the distribution is normalized with the condition $2\pi\int p\big(|\epsilon^{\rm s}|\big)|\epsilon^{\rm s}|\,{\rm d}|\epsilon^{\rm s}| = 1$. Galaxy positions are chosen randomly on the field. For simplicity, following Seitz & Schneider (1996), we take a uniform distribution in the *observed* position, thus neglecting magnification effects. Finally, following Brainerd et al. (1996), we draw the redshifts from a gamma distribution

$$p_z(z) = \frac{z^2}{2z_0^3}\exp(-z/z_0)\ , \qquad (33)$$

where $z_0 = 2/3$. This distribution has maximum at $z = 2z_0 = 4/3$ and mean $\langle z\rangle = 3z_0 = 2$. Current surveys favor a slightly higher value of z_0 (Driver et al. 1998, for a limiting magnitude $I < 26$). All distributions can be obtained from a uniform distribution by the transformation or rejection methods (see Press et al. 1992).

Then the observed galaxy ellipticities are calculated using Eq. (12). The "observations" used for the reconstruction process are then the set of galaxy positions $\big\{\boldsymbol{\theta}^{(n)}\big\}$, the set of observed ellipticities $\big\{\epsilon^{(n)}\big\}$, and the set of redshifts $\big\{z^{(n)}\big\}$. The simulations are carried out with Gaussian weights in $\|\boldsymbol{\theta}-\boldsymbol{\theta}'\|$ (with scale lenght $9''$) and in $|z-z'|$ (with scale 0.2).

The reconstruction process follows the method described in Sect. 3, and can be summarized in 9 steps:

1. To begin the reconstruction, an Einstein-de Sitter universe is assumed, and thus, as first guess, the cosmological weight $w^{[0]}(z)$ is calculated (Eq. (8)).
2. The initial density $\kappa^{[0,0]}$ and the initial shear $\gamma^{[0,0]}$ are both set to zero.
3. A first determination of the shear $\gamma^{[0,1]}(\boldsymbol{\theta})$ is then obtained from the observed ellipticities using Eq. (20).
4. The new mass distribution $\kappa^{[0,1]}(\boldsymbol{\theta})$ is calculated using the shear $\gamma^{[0,1]}(\boldsymbol{\theta})$. The inversion from the shear into the mass distribution is performed by convolution with the curl-free kernel $\boldsymbol{H}^{\rm SS}(\boldsymbol{\theta},\boldsymbol{\theta}')$ (Seitz & Schneider 1996; for a discussion on the merits of different kernels see Paper II). The sheet invariance is broken by requiring the total reconstructed mass $\int\kappa(\boldsymbol{\theta})\,{\rm d}^2\theta$ to be equal to the true value (see Sect. 4.3).

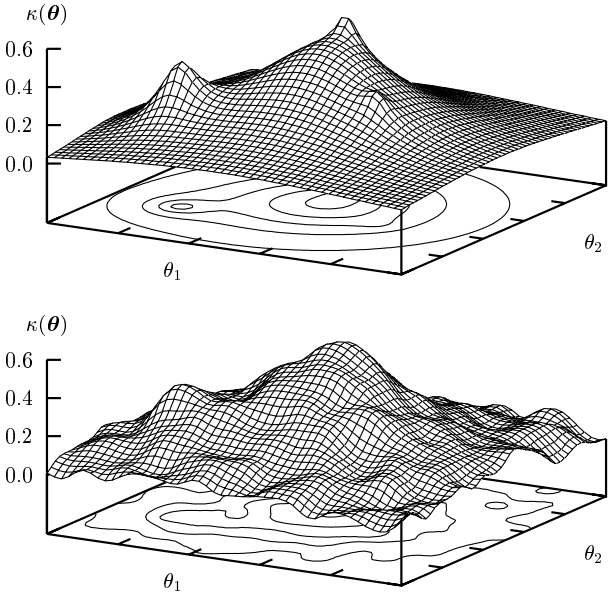

Fig. 2. The original dimensionless mass density and an example of reconstruction. The number of galaxies used is $N = 20\,000$; the assumed cosmological model is Einstein-de Sitter. The cluster occupies a square with side of $5'$, corresponding approximately to $1.23\,h^{-1}$Mpc.

5. Points (2), (3), and (4) are iterated. This is repeated a number I of times sufficient to obtain good convergence (typically $I = 5$ for sub-critical clusters).
6. The final determinations $\kappa^{[0,I]}$ and $\gamma^{[0,I]}$ are used in Eq. (21) to get the new weight function $w^{[1]}$.
7. Points (2–5) are iterated, thus leading to the determination of $w^{[j+1]}$ from the knowledge of $w^{[j]}$. (The *outer iteration* on j involves w, while the *inner iteration* on i involves κ and γ.) As starting density and shear for the new inner iteration we use the last determinations of these quantities, i.e. $\kappa^{[j+1,0]} = \kappa^{[j,I]}$ and similarly $\gamma^{[j+1,0]} = \gamma^{[j,I]}$. The outer iteration is performed a number J of times.
8. The final lens density $\kappa^{[J,I]}$ is then compared to the true one κ_0.
9. The final cosmological weight $w^{[J]}$ is then used to determine, or at least constrain, the geometry of the universe. The methods used are the ones described in detail in Appendix D.

Simulations show that, for "reasonable" values of Ω and Ω_Λ, the factor k related to the global scaling invariance remains very close to unity; thus the measured cosmological weight does not differ significantly from the true cosmological weight. This happens because the cosmological weight changes only slightly for different values of Ω and Ω_Λ (cfr. Fig. 1). Hence the initial choice $w^{[0]}(z)$ (Einsten-de Sitter universe) is not far from the true $w_0(z)$. In this situation it is correct to use the measured total mass to break the sheet invariance, as done in point 4 (instead, in the presence of a wrong scaling factor k, this procedure might lead to undesired results because of the coupling of the sheet invariance with the global scaling invariance).

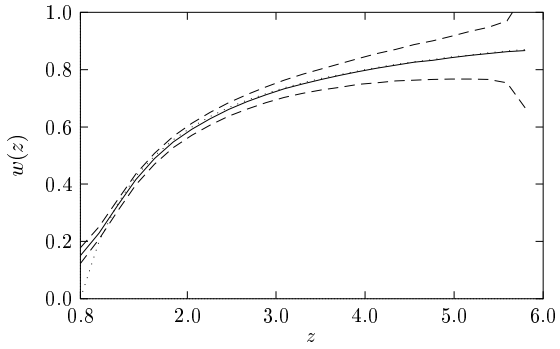

Fig. 3. The weight expected mean and error on the weight function for an Einstein-de Sitter universe. The solid line shows $\langle w\rangle(z)$, the dashed lines the expected errors (obtained as $\sqrt{\mathrm{Cov}(w;z,z)}$) and the dotted line the true $w_0(z)$. The errors are calculated for $N = 10\,000$ galaxies; errors for different values of N can be obtained by recalling that the error scales as $\sqrt{N}$.

6.2. Results

A wide set of simulations show that the method produces significant results if the number of galaxies studied is a few thousand or more.

The first part of the reconstruction deals with the shear $\gamma(\boldsymbol{\theta})$ and with the mass distribution $\kappa(\boldsymbol{\theta})$. Fig. 2 shows an example of mass density obtained from the method. The map obtained is rather detailed and smooth because of the large number of galaxies used ($N = 20\,000$). As explained in detail in Paper II, these properties depend on the spatial weight function $W(\boldsymbol{\theta},\boldsymbol{\theta}')$ used: the larger the characteristic size of this function, the smoother the shear and density maps obtained. This behavior is consistent also with the calculations of Appendix C. In the simulations this size has been adjusted to the value that gives the best results on the following discussion of the cosmological parameters.

The initial guess for the cosmological weight function $w^{[0]}$ is not very important for the determination of the shear, because a wrong choice would only lead to an increase of the errors (at least in the weak lensing limit; see comment after Eq. (C4)). This behavior is well verified in the simulations. At the end of the first inner iteration, the mass density obtained, $\kappa^{[0,I]}$, does not differ significantly from the determinations obtained at the end of the following cycles, $\kappa^{[j,I]}$ (except for a factor arising from the global scaling invariance). After the first inner cycle, the mass and the shear maps are close to the best ones that we can hope to have. This suggests that the number of inner iterations I could decrease after the first cycle. Thus we could start with $I = 5$ for $j = 0$, and then let $I = 3$ or even $I = 2$ for $j > 0$. The reduction of I can lead to a significant reduction of machine-time.

The following step is the determination of the cosmological weight. Simulations show that the number of outer iterations needed to obtain a good estimation of the cosmological weight is very low, say $J = 3$, because the method is able to give the correct shear map after the first inner loop. Simulations also show that this property, strictly expected only in the weak lensing limit, is in fact valid (at least approximately) in the general

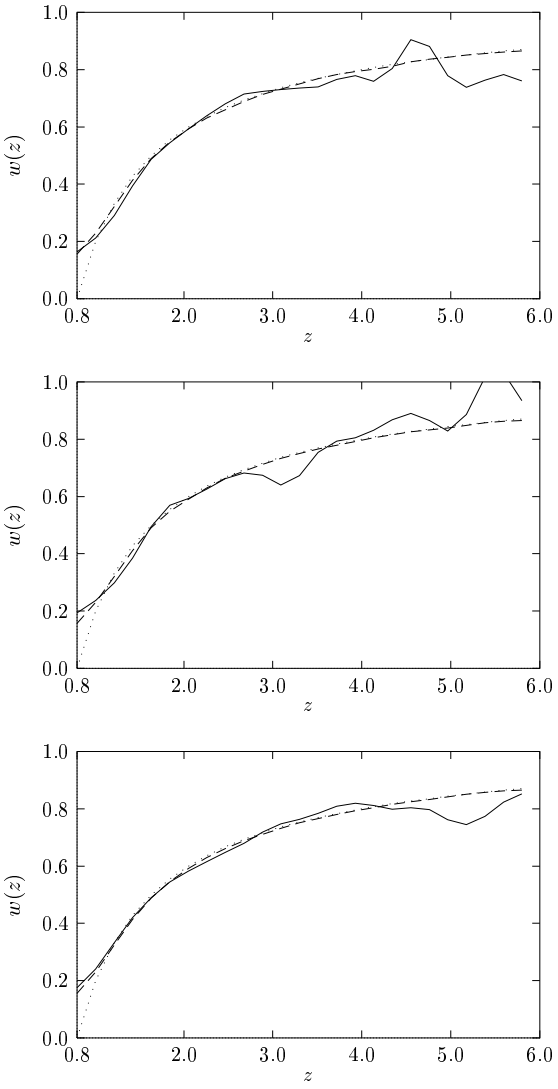

Fig. 4. The reconstructed weight function in an Einstein-de Sitter universe ($\Omega = 1$, $\Omega_\Lambda = 0$). The dotted line represent the true weight function $w_0(z)$; the dashed line is the expected mean value $\langle w\rangle(z)$, as predicted by Eq. (C7); the solid line is the measured $\hat{w}(z)$. The three figures have been obtained with $N = 10\,000$ (*top*), $N = 20\,000$ (*middle*) and $N = 50\,000$ (*bottom*) of source galaxies.

case, provided the lens is not too "strong." The estimated cosmological weight $\hat{w}(z)$ (solid lines in Fig. 4) is smooth on the characteristic scale of $W_z(z,z')$ (see Eq. (C7)); because of this, it remains at a finite value at $z = z_\mathrm{d}$. Moreover, as expected, the error on the cosmological weight increases slightly for z near z_d and more for high values of z, where the number of galaxies decreases (see Fig. 3). In particular, the smoothing of the cosmological weight is very important near the cluster, at $z \simeq z_\mathrm{d}$, where the true cosmological weight vanishes abruptly. This clearly indicates that neither the limit $w(z) \to 1$ for $z \to \infty$ nor the limit for $z \to z_\mathrm{d}^+$ can be used to break the global scaling invariance. Fig. 4 shows the reconstruction of the cosmological weight in the case of an Einstein-de Sitter universe; different choices for Ω and Ω_Λ lead to similar results. Fig. 4 should be

compared with Fig. 3 which shows the expected mean value $\langle w\rangle(z)$ and the related error for an Einstein-de Sitter universe with $N = 10\,000$ galaxies. Fig. 3 clarifies the general properties discussed above and, in more detail, in Appendix D, for the expected error on $w(z)$ and suggests that our method should be able to constrain significantly the cosmological parameters. In fact, the error on $w(z)$ for $z \simeq 2$ is sufficiently small to distinguish different consmological models even if the measured weight are affected by the global scaling invariance.

From the estimation $\hat{w}(z)$ of the cosmological weight we can obtain information on the cosmological parameters as explained in Appendix D. For a description of the results, we plot the contours of the ℓ_2 function of Eq. (D6) in a square domain $[0,1] \times [0,1]$ of the Ω-Ω_Λ plane. Figs. 5 and 6 show the confidence regions obtained for various confidence levels CL in different cosmological models and with different numbers of source galaxies. From diagrams of this type we argue that $N = 10\,000$ can be considered as a lower bound for the applicability of our method.

These figures also show that, unless an exceedingly high number of source galaxies is available, point estimation is not very meaningful. In fact, these examples show that the minimum of the χ^2 function can occur quite far from the true values of the cosmological parameters. On the other hand, for not unreasonable (see discussion in Sect. 7) values of N, the method does *constrain* the cosmological parameters. If additional a priori conditions are included (e.g., if the universe is taken to have $\Omega_\Lambda = 0$), parameters can be constrained rather efficiently.

In order to check the distribution of ℓ_2, we have repeated a large number of times the entire process, using each time a different set of source galaxies. The measured probability distribution of ℓ_2 for different values of N is shown in Figs. 7 and 8. In these figures, the histograms show the number of simulations that have produced a value of ℓ_2 in the corresponding interval. Intervals are chosen so that the theoretical number of events per bin is constant. From these and other results not shown it is clear that ℓ_2 tends to a chi-square distribution with two degrees of freedom only for a very large number of galaxies N, say $N \gtrsim 100\,000$. In contrast, for "small" values of N the observed distribution is (approximately) consistent with a chi-square with one degree of freedom. This suggests that, when the number of galaxies is small, a new approximate invariance may be present. The method is able to break this invariance for larger values of N.

This behavior is also suggested by the shapes of the confidence regions of Figs. 5 and 6. In fact, the confidence regions obtained have a characteristic shape approximately following the lines $\Omega + \Omega_\Lambda = 1 - \Omega_R = \text{const}$. Thus our method should be able to constrain well the curvature Ω_R, while the quantity $\Omega - \Omega_\Lambda$ should remain practically unknown, at least when the number N of galaxies used is not too high. This approximate invariance may explain the behavior of the quantity ℓ_2 for finite N. In fact, if the invariance were exact, ℓ_2 would be expected to follow a chi-square distribution with (only) one degree of freedom. This is indeed observed for $N \lesssim 50\,000$. Thus in order to draw the confidence regions, one should use the results of Monte Carlo simulations, unless the number N of galaxies is *very* large. The contours presented in this paper have been obtained from Monte Carlo simulations. The use of the asymptotic limit would have led indeed to *larger* confidence regions.

7. Feasibility

In this section we briefly discuss the applicability of our method to observations. As noted earlier, the main difficulty with our method is probably the high number of galaxies (and redshifts) needed to obtain significant constraints on the geometry of the universe.

In order to show that the examples chosen for our simulations can be considered to be not unrealistic, we first note that the required density of galaxies is between 400 and 800 galaxies per square arcminute. This density is certainly too high for current instruments. In fact, the current achievable density of galaxies (with "reasonable" integration times) is of the order of 60 galaxies per square arcminute (Clowe et al. 1998), and this number is only likely to double with the Advanced Camera on HST. However, current estimates for NGST (Stiavelli et al. 1997) give more than $1\,000$ galaxies per square arcminute. It is also interesting to note that the baseline for the camera currently considered for NGST is about $4'$, not far from the value used in our simulations ($5'$).

A second difficulty with the method proposed here is the large number of redshifts required. As suggested in the Introduction, photometric redshifts might be used. In this case, however, sizable statistical errors on the measured redshifts are expected. At this stage, for simplicity, such errors have not been taken into account in the simulations, but they obviously should be considered in detail before applications are tried. (We note also that errors on the measurement of ellipticities may have an impact, especially if small and weak source galaxies are used.)

Another important ingredient is the cluster chosen in our simulations. In an Einstein-de Sitter universe with $h = 0.5$, the cluster would have a mass within a 1 Mpc aperture of about $2\times10^{15}\,\mathrm{M}_\odot$. We may compare our cluster with the X-ray cluster MS $1054-03$ located at $z_d = 0.83$ (Luppino & Kaiser 1997); weak lensing estimates for this cluster give a mass within 1 Mpc in the range $1.2 \times 10^{15}\,\mathrm{M}_\odot$ and $5.5 \times 10^{15}\,\mathrm{M}_\odot$, depending on the assumed redshift distribution for the source galaxies.

In conclusion, the proposed method should give interesting results if applied to NGST observations. Of course, several refinements and improvements would be required for the purpose. For example, as suggested in the Introduction, the use of several clusters should provide tighter constraints on the cosmological parameters. Broadly speaking, the use of N_{cl} similar clusters should make the errors on the cosmological parameters smaller by a factor $\sqrt{N_{\mathrm{cl}}}$. However, for this purpose the method should be generalized to be applied to different clusters at different redshifts (actually, we expect that if the redshifts of the clusters are different, more information on the geometry of the universe is available). We should also keep in mind that, intuitively, the use of several clusters may introduce additional difficulties, much like the case of a single cluster with pronounced substructure.

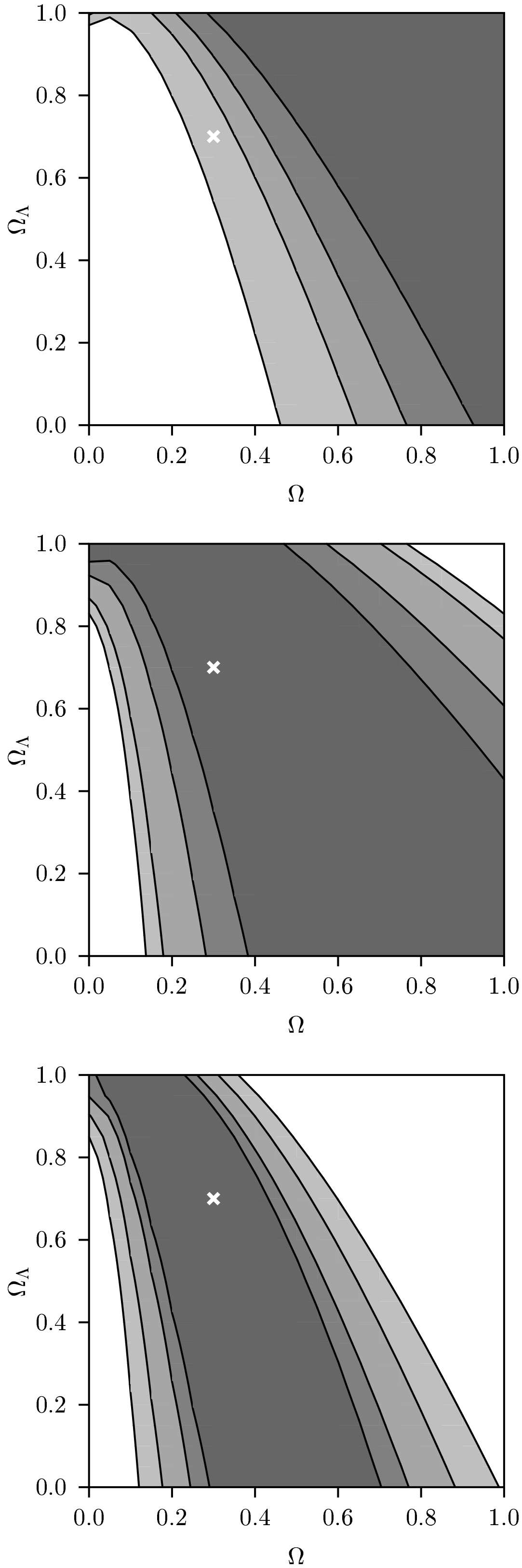

Fig. 5. The confidence regions corresponding to $CL = 68\%$, $CL = 80\%$, $CL = 90\%$ and $CL = 95\%$. The true value of the cosmological parameters, $\Omega = 0.3$ and $\Omega_\Lambda = 0.7$, is shown as a white cross. The galaxies used are $N = 10\,000$ (*top*), $N = 20\,000$ (*middle*) and $N = 50\,000$ (*bottom*).

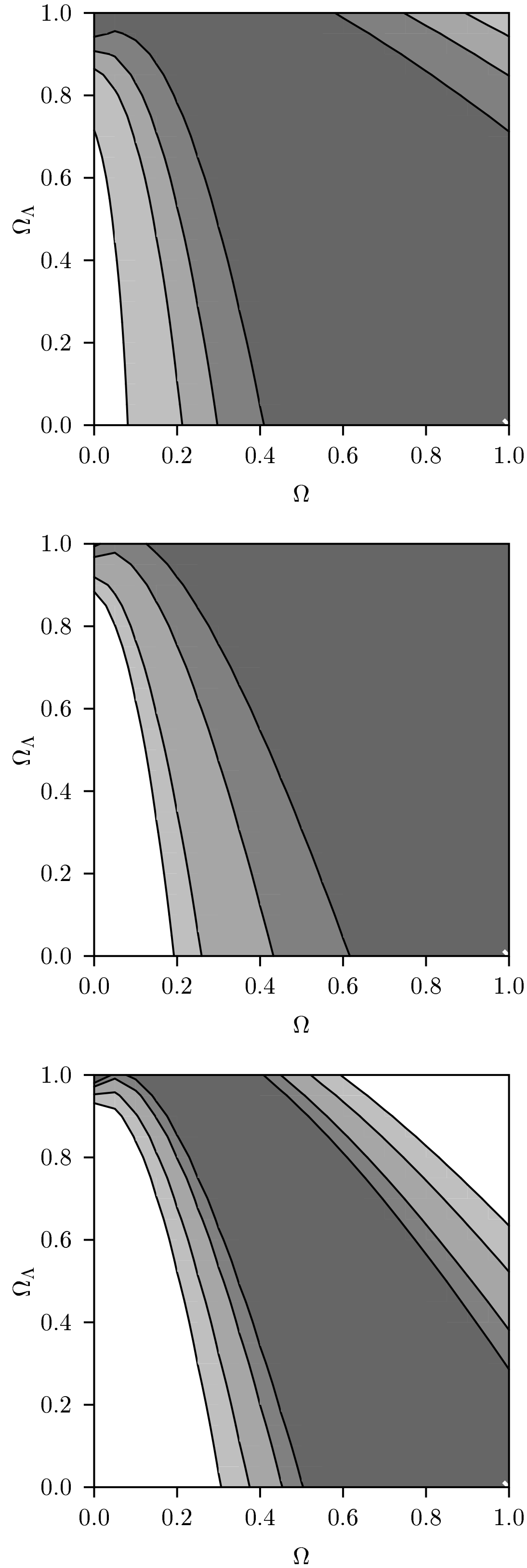

Fig. 6. As Fig. 5, but with $\Omega = 1$ and $\Omega_\Lambda = 0$.

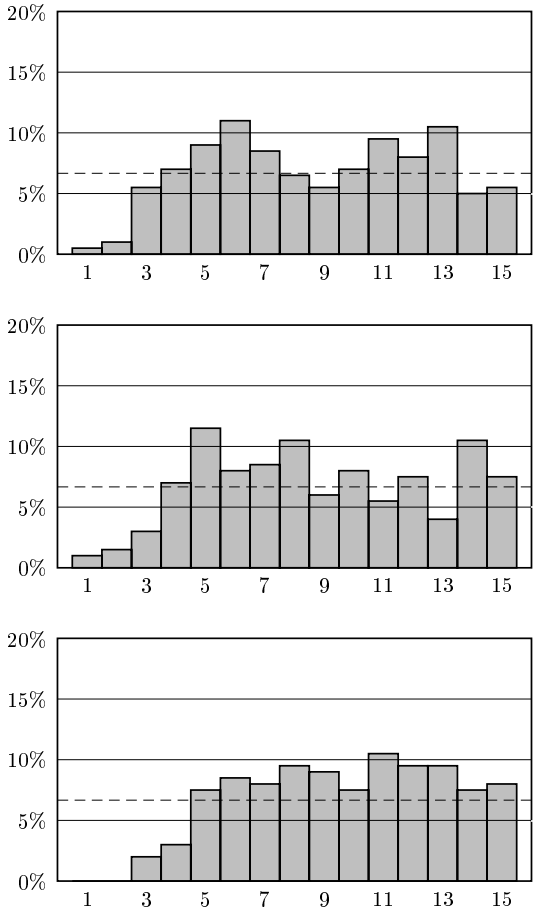

Fig. 7. The observed probability distribution for ℓ_2. The 15 bins have been chosen so that the expected number of events per bin would be constant if ℓ_2 followed a chi-square distribution with *one* degree of freedom. The graphs show that, except for the first two bins, the observed probability distribution is roughly constant. The three graphs correspond to $N = 10\,000$ (*top*), $N = 20\,000$ (*middle*), and $N = 50\,000$ (*bottom*).

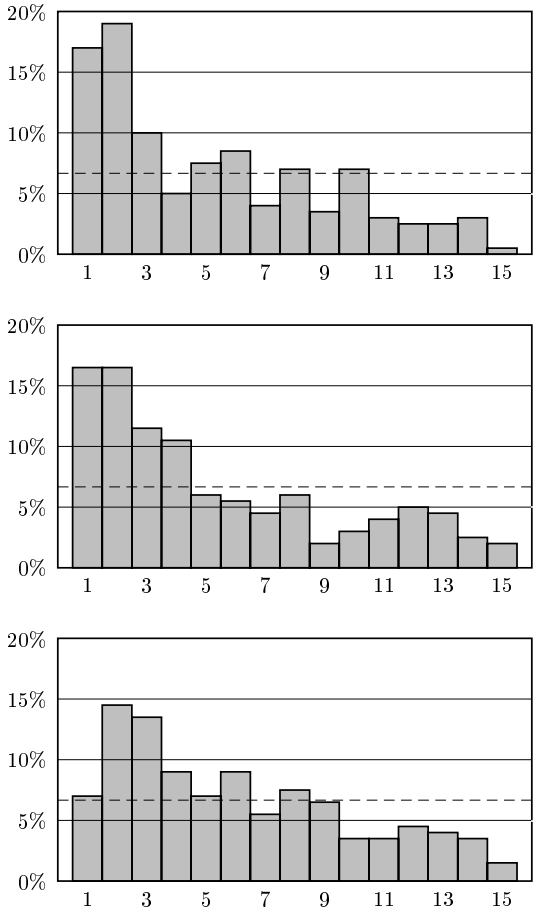

Fig. 8. As for Fig. 7, but with bins chosen so that the expected number of events per bin would be constant if ℓ_2 followed a chi-square distribution with *two* degrees of freedom.

Finally, we should stress that a potential problem for the application of our method could be that of multiple lensing. In fact, if weak lensing analysis is used (in order to solve the problem of the sheet invariance), "tidal" effects of other clusters (or from large scale structures) could become important and may jeopardize the applicability of the method. On the other hand, it is often very hard to break the sheet invariance. In view of the above considerations, it would be very interesting to develop a method able to overcome these problems, possibly by decoupling the sheet and the global scaling invariance properties.

8. Conclusions

In this paper we have proposed and discussed a method, based on weak lensing and redshift observations, to reconstruct the lens mass distribution and to obtain, at the same time, information on the geometry of the universe. Simulations based on the homogeneous Friedmann-Lemaître models have shown that the method is viable when the number of source galaxies is sufficiently high. In principle, the same method could be extended to other cosmological models, provided that the angular diameter-distance relation be available; some of these would be harder to handle because they involve a larger number of free parameters (e.g., the inhomogeneous "in average" Friedmann-Lemaître models; see Kayser et al. 1997).

In this paper we have used a "parameter-free" approach in the determination of the cosmological weight. In fact, in the reconstruction process we have tried to determine the values of $w(z)$ for a number of different redshifts (25 in our simulations), without any assumption on its shape. A different method could have been used, namely the direct determination of the cosmological parameters without the intermediate determination of the cosmological weight $w(z)$ (parametric approach). In this case the cosmological parameters could have been estimated using, for example, a maximum likelihood method. A similar dichotomy exists between parametric and non-parametric mass reconstructions. We have decided to use here the non-parametric approach as more "conservative," but it would be interesting to develop a parametric method in detail for comparison.

One improvement that could be made on the current method is based on more direct use of the shear in the determination of

the cosmological weight (see Eq. (18)). In fact, the complex shear $\gamma(\boldsymbol{\theta})$ is not an independent quantity, in the sense that a relation between its partial derivatives holds (i.e., $\nabla \wedge \boldsymbol{u}(\boldsymbol{\theta}) = 0$; see Paper II for a detailed discussion). Hence it is natural to expect that the inclusion of an additional relation, not considered in the present paper, could improve the determination of $w(z)$. This might be implemented by resorting to a maximum likelihood approach for the measurement of the shear map.

Acknowledgements. It is a pleasure to thank Peter Schneider for several suggestions that have helped us improve the paper. This work has been partially supported by MURST and by ASI of Italy. The simulations have been performed on a Digital Alpha LX164 running at 533 MHz.

Appendix A: the sheet invariance

In this Appendix we describe the sheet invariance for non-weak lenses. Our discussion largely follows Seitz & Schneider (1997).

Following the approach of Appendix C, we start by taking a fixed cosmological weight equal to the true cosmological weight times a given constant, i.e. $w(z) = \nu w_0(z)$. By using a global scaling invariance with scaling factor $k = 1/\nu$ we can make $w(z) = w_0(z)$. An approximate expression for the mean value of the measured shear, valid also for non-weak lenses, can be shown to be

$$\langle\gamma\rangle \simeq \frac{\langle w\rangle_z - \kappa\langle w^2\rangle_z}{\langle w\rangle_z - \kappa_0\langle w^2\rangle_z}\gamma_0 \ . \tag{A1}$$

In this equation we have neglected the smoothing effect of the weight function $W(\boldsymbol{\theta}, \boldsymbol{\theta}')$. From this relation we can derive the form of the sheet invariance. Suppose that $\langle\gamma\rangle = (1-C)\gamma_0$, with C constant. This simply means that the measured value of γ is proportional to the true shear. Then the previous equation gives

$$\kappa = \frac{C\langle w\rangle_z}{\langle w^2\rangle_z} + (1-C)\kappa_0 \ . \tag{A2}$$

This equation is consistent with the assumption $\gamma = (1-C)\gamma_0$ because the "sheet constant" $C\langle w\rangle_z/\langle w^2\rangle_z$ does not affect the shear. Eq. (25) thus gives the form of the sheet invariance for the dimensionless projected density κ in the general case.

If we use these relations in Eq. (21) we can derive the expected transformation induced on the measurement of the cosmological weight. The expressions obtained, rather complicated, are not reported here. However it is clear that the cosmological weight *changes*, i.e. the measured $w(z)$ is different from $w_0(z)$. Moreover, it can be shown that $w(z)/w_0(z)$ is not constant: this of course means that the sheet invariance has a different effect on the cosmological weight with respect to the global scaling invariance.

Appendix B: a constraint on the total projected mass of the lens

The goal of this Appendix is to prove Eq. (27) (following Lombardi 1996). As a first step we note that

$$\int \big[1 - \det A(\boldsymbol{\theta})\big]\,\mathrm{d}^2\theta \ = \ \lim_{R\to\infty}\int_{B_R}\big[1 - \det A(\boldsymbol{\theta})\big]\,\mathrm{d}^2\theta$$
$$= \ \lim_{R\to\infty}\left(\int_{B_R}\mathrm{d}^2\theta - \int_{\boldsymbol{\theta}^{\mathrm{s}}(B_R)}\mathrm{d}^2\theta^{\mathrm{s}}\right) . \tag{B1}$$

In this equation B_R is the disk of radius R centered in the origin of the $\boldsymbol{\theta}$-plane, while $\boldsymbol{\theta}^{\mathrm{s}}(B_R)$ is the image, through the ray-tracing function $\boldsymbol{\theta}^{\mathrm{s}}(\boldsymbol{\theta})$, of the disk B_R. The second equality holds because of the change of variable formula.

A well-known property of gravitational lenses is that the deflection $\boldsymbol{\beta}(\boldsymbol{\theta}) = \boldsymbol{\theta}^{\mathrm{s}}(\boldsymbol{\theta}) - \boldsymbol{\theta}$ can be expressed as the gradient of the deflection potential $\psi(\boldsymbol{\theta})$ (given the symmetry of the Jacobian matrix A of Eq. (9)). Such potential can be written as

$$\psi(\boldsymbol{\theta}) = \frac{1}{\pi}\int \kappa(\boldsymbol{\theta}')\ln\|\boldsymbol{\theta} - \boldsymbol{\theta}'\|\,\mathrm{d}^2\theta' \ . \tag{B2}$$

For an isolated distribution of matter, such that the mass density κ vanishes outside a given disk B_R, the potential can be expressed (outside B_R) in terms of a multipole expansion

$$\psi(\boldsymbol{\theta}) = \frac{1}{\pi}\left(M\ln\theta - \frac{\boldsymbol{p}\cdot\boldsymbol{\theta}}{\theta^2} - \frac{1}{2}\sum_{ij}\frac{q_{ij}\theta_i\theta_j}{\theta^4} - \cdots\right) , \tag{B3}$$

where

$$M \ = \ \int \kappa(\boldsymbol{\theta}')\,\mathrm{d}^2\theta' \ , \tag{B4}$$

$$p_i \ = \ \int \theta'_i\kappa(\boldsymbol{\theta}')\,\mathrm{d}^2\theta' \ , \tag{B5}$$

$$q_{ij} \ = \ \int (2\theta'_i\theta'_j - \delta_{ij}\theta'^2)\kappa(\boldsymbol{\theta}')\,\mathrm{d}^2\theta' \ . \tag{B6}$$

(The first physically important term after M is the quadrupole q_{ij}, as the dipole p_i vanishes if the origin of axes is chosen in a suitable way.) Thus we obtain for the deflection

$$\boldsymbol{\beta}(\boldsymbol{\theta}) = \nabla\psi(\boldsymbol{\theta}) = \frac{1}{\pi}\left(\frac{M\boldsymbol{\theta}}{\theta^2} - \frac{\boldsymbol{p}}{\theta^2} + \frac{2(\boldsymbol{p}\cdot\boldsymbol{\theta})\boldsymbol{\theta}}{\theta^4} + \cdots\right) . \tag{B7}$$

Using this expression we can estimate the last integral in Eq. (B1). In fact, using the definition of $\boldsymbol{\beta}(\boldsymbol{\theta})$ and neglecting terms of order $\mathcal{O}\big(\theta^{-2}\big)$, we can say that the region $\boldsymbol{\theta}^{\mathrm{s}}(B_R)$ is a disk of radius

$$R^{\mathrm{s}} = R - \frac{M}{\pi R} \ . \tag{B8}$$

Thus we find

$$\int_{\boldsymbol{\theta}^{\mathrm{s}}(B_R)}\mathrm{d}^2\theta \ = \ \pi\left(R - \frac{M}{\pi R}\right)^2 + \mathcal{O}\big(R^{-1}\big)$$
$$= \ \pi R^2 - 2M + \mathcal{O}\big(R^{-1}\big) \ . \tag{B9}$$

Inserting this expression in Eq. (B1), we obtain Eq. (27). A more detailed discussion shows that, in reality, the error involved is not $\mathcal{O}\big(R^{-1}\big)$ but $\mathcal{O}\big(R^{-2}\big)$, and precisely it is of order $\mathcal{O}\big(M^2/R^2, q/R^2\big)$. This property has to do with the fact that the dipole $\boldsymbol{p}$, which would be responsible for the error of order $\mathcal{O}\big(R^{-1}\big)$, can be made to vanish with a suitable choice of the origin of the axes. However, the origin of coordinates is not important when we take the limit $R \to \infty$, and thus the error is only of order $\mathcal{O}\big(R^{-2}\big)$.

An improved version of Eq. (27) can be obtained by retaining the term of order $\mathcal{O}(M^2/R^2)$:

$$\frac{1}{2}\int_{B_R}\left[1-\det A(\boldsymbol{\theta})\right]\mathrm{d}^2\theta \simeq M-\frac{M^2}{2\pi R^2}\ . \tag{B10}$$

This expression may become useful when the quadrupole q_{ij} is neglegible.

Appendix C: expectation values and errors

An analytic calculation of the expectation values and errors for the shear and for the cosmological weight is important both for a first check of the quality of our method and for its practical implementation. The problem is not easy to solve in the general case, mainly because it involves iterations of different equations. For this reason we will often simplify the discussion by introducing some approximations.

We expect calculations for the covariance matrix of $\hat{w}$ to be especially difficult, mainly because in Eq. (18) for $\hat{w}(z)$ the quantity $\gamma(\boldsymbol{\theta})$ has been calculated using the *same* galaxies to be used for $w(z)$. Thus the errors on $\hat{w}$ and on $\hat{\gamma}$ should be correlated. (Strictly speaking this is true also for the covariance matrix of $\hat{\gamma}$, but such dependence is not very important for our problem.) For simplicity, in the following we will consider either the cosmological weight or the shear map fixed in the calculation of the expectation value and error of the other quantity. The results obtained, checked by simulations, show that this approximation is good.

The general method used for calculating expectation values and errors is described in detail in Paper I and Paper II (see especially Appendix C of the latter article) and is based on the assumption that we can linearize the relevant equations near the mean value of the random variables. Calculations will be done by replacing summations with integrals, so that Poisson noise will be neglected. As explained in Paper II, Poisson noise generally adds only a small correction to the dominant sources of error. For this purpose we define the redshift probability distribution $p_z(z)$. Hence the probability that a galaxy is observed in the solid angle $\mathrm{d}^2\theta$ and with redshift in the range $[z, z+\mathrm{d}z]$ is given by $\rho p_z(z)\,\mathrm{d}^2\theta\,\mathrm{d}z$ (notice that source galaxies are taken to be uniformly distributed on the field, and thus ρ does not depend on $\boldsymbol{\theta}$). In the following, for simplicity, we will also assume that the distribution of source ellipticities is independent of redshift.

C.1. Weak lensing

C.1.1. Expectation values

Calculations are not difficult in the weak lensing limit because all expressions are linear. The shear is calculated from Eq. (17), and thus, from Eq. (16), the expected value of the shear is

$$\langle\hat{\gamma}\rangle(\boldsymbol{\theta}) = \frac{\sum_{n=1}^{N} W\big(\boldsymbol{\theta},\boldsymbol{\theta}^{(n)}\big)w\big(z^{(n)}\big)w_0\big(z^{(n)}\big)\gamma_0\big(\boldsymbol{\theta}^{(n)}\big)}{\sum_{n=1}^{N} W\big(\boldsymbol{\theta},\boldsymbol{\theta}^{(n)}\big)\big[w\big(z^{(n)}\big)\big]^2}\ . \tag{C1}$$

If we move to a continuous distribution we find

$$\begin{aligned}\langle\hat{\gamma}\rangle(\boldsymbol{\theta}) \;=\; &\left[\int\mathrm{d}^2\theta'\int\mathrm{d}z'\,p_z(z')W(\boldsymbol{\theta},\boldsymbol{\theta}')w(z')w_0(z')\times\right.\\ &\left.\times\,\gamma_0(\boldsymbol{\theta}')\right]\left[\int\mathrm{d}^2\theta'\int\mathrm{d}z'\,W(\boldsymbol{\theta},\boldsymbol{\theta}')\times\right.\\ &\left.p_z(z')\big[w(z')\big]^2\right]^{-1}\ .\end{aligned} \tag{C2}$$

We observe now that the integrals on $\mathrm{d}^2\theta'$ and on $\mathrm{d}z'$ factorize, thus leaving simply

$$\langle\hat{\gamma}\rangle(\boldsymbol{\theta}) = K\frac{\int\mathrm{d}^2\theta'\,W(\boldsymbol{\theta},\boldsymbol{\theta}')\gamma_0(\boldsymbol{\theta}')}{\int\mathrm{d}^2\theta'\,W(\boldsymbol{\theta},\boldsymbol{\theta}')}\ . \tag{C3}$$

The constant K is obviously related to the global scaling invariance and is given by

$$K=\frac{\int\mathrm{d}z'\,p_z(z')w(z')w_0(z')}{\int\mathrm{d}z'\,p_z(z')\big[w(z')\big]^2}\ . \tag{C4}$$

Note that K is $\boldsymbol{\theta}$-independent, so that the use of an inaccurate cosmological weight affects only the scale of the expected measured shear. A result similar to Eq. (C3) has been obtained in Paper II.

From Eq. (18), the expectation value of the cosmological weight is given by

$$\begin{aligned}&\langle\hat{w}\rangle(z)\\ &=\frac{\sum_{n=1}^{N} W_z\big(z,z^{(n)}\big)\Re\big[w_0\big(z^{(n)}\big)\hat{\gamma}\big(\boldsymbol{\theta}^{(n)}\big)\gamma_0^*\big(\boldsymbol{\theta}^{(n)}\big)\big]}{\sum_{n=1}^{N} W_z\big(z,z^{(n)}\big)\big|\hat{\gamma}\big(\boldsymbol{\theta}^{(n)}\big)\big|^2}\ .\end{aligned} \tag{C5}$$

By moving to a continuous distribution and by replacing $\hat{\gamma}$ with its expected value given by Eq. (C3), we obtain

$$\begin{aligned}\langle\hat{w}\rangle(z) \;=\; &\frac{1}{K}\left[\int\mathrm{d}z'\int\mathrm{d}^2\theta'\,p_z(z')W_z(z,z')w_0(z')\times\right.\\ &\left.\Re\left(\int\mathrm{d}^2\theta''\,W(\boldsymbol{\theta}',\boldsymbol{\theta}'')\gamma_0^*(\boldsymbol{\theta}')\gamma_0(\boldsymbol{\theta}'')\right)\right]\times\\ &\times\left[\int\mathrm{d}z'\int\mathrm{d}^2\theta'\,p_z(z')W_z(z,z')\right.\\ &\left.\left|\int\mathrm{d}^2\theta''\,W(\boldsymbol{\theta}',\boldsymbol{\theta}'')\gamma_0(\boldsymbol{\theta}'')\right|^2\right]^{-1}\ .\end{aligned} \tag{C6}$$

As for the shear the integrals on the redshift factorize. Let us consider in more detail the integrals on the angles, i.e. $\Re(\cdots)$ in the numerator and $\int\mathrm{d}^2\theta'\int\mathrm{d}^2\theta''|\cdots|^2$ in the denominator. These two quantities differ only by one integration with weight $W(\boldsymbol{\theta}',\boldsymbol{\theta}'')$. Thus we may argue that

$$\langle\hat{w}\rangle(z)\simeq\frac{1}{K}\frac{\int\mathrm{d}z'\,p_z(z')W_z(z,z')w_0(z')}{\int\mathrm{d}z'\,p_z(z')W_z(z,z')}\ . \tag{C7}$$

We note that here the constant K appears at the denominator, consistent with the global scaling invariance.

In the following, in order to simplify equations, we will introduce the normalization condition

$$\int\mathrm{d}z'\,p_z(z')W_z(z,z')=1\quad\forall z\ . \tag{C8}$$

Similarly, we will consider the angular weight functions (see Eq. (C3)) to be normalized, i.e. to satisfy the condition

$$\rho \int W(\boldsymbol{\theta}, \boldsymbol{\theta}')\, \mathrm{d}^2\theta' = 1 \quad \forall \boldsymbol{\theta}\ . \tag{C9}$$

We recall that this does not limit our discussion, since only *relative* values of W are important (see Paper II).

C.1.2. Errors

Let us now consider the error (i.e. the covariance matrix) of $\hat{\gamma}$. Using the definitions of Paper I and Paper II and calling ϵ_1 and ϵ_2 the real and imaginary components of the ellipticity ϵ, we find

$$\mathrm{Cov}(\hat{\gamma}; \boldsymbol{\theta}, \boldsymbol{\theta}') = \sum_{n=1}^{N} \left(\frac{\partial \hat{\gamma}(\boldsymbol{\theta})}{\partial \epsilon^{(n)}} \right) \mathrm{Cov}\big(\epsilon^{(n)}\big) \left(\frac{\partial \hat{\gamma}(\boldsymbol{\theta}')}{\partial \epsilon^{(n)}} \right)^{\mathrm{T}} . \tag{C10}$$

In this equation we have used the matrix notation for the partial derivatives. For example, the last matrix, because of the transpose, has $\partial \hat{\gamma}_j(\boldsymbol{\theta}')/\partial \epsilon_i^{(n)}$ in the element with row i and column j. From Eq. (15) we find that $\mathrm{Cov}(\epsilon) = \mathrm{Cov}(\epsilon^{\mathrm{s}}) = c\,\mathrm{Id}$, where c is a positive constant and Id is the 2×2 identity matrix (note that, as the source ellipticities are taken to be independent of redshift, c is independent of redshift as well). The partial derivatives of $\hat{\gamma}$ can be calculated from Eq. (17). By moving to the continuous description, after some manipulations we find

$$\mathrm{Cov}(\hat{\gamma}; \boldsymbol{\theta}, \boldsymbol{\theta}') = c\rho \frac{\int \mathrm{d}^2\theta''\, W(\boldsymbol{\theta}, \boldsymbol{\theta}'') W(\boldsymbol{\theta}', \boldsymbol{\theta}'')}{\int \mathrm{d}z''\, p_z(z'') \big[w(z'')\big]^2}\, \mathrm{Id}\ , \tag{C11}$$

where the normalization condition (C9) has been used. This result is a generalization of a similar result obtained in Paper II (see Eq. (26) of that article).

If we consider γ fixed, the covariance matrix of $\hat{w}$ is given by

$$\begin{aligned} \mathrm{Cov}(\hat{w}; z, z') \ = \ & \sum_{n=1}^{N} \left(\frac{\partial \hat{w}(z)}{\partial \epsilon^{(n)}} \right) \mathrm{Cov}_{ij}\big(\epsilon^{(n)}\big) \\ & \times \left(\frac{\partial \hat{w}(z')}{\partial \epsilon^{(n)}} \right)^{\mathrm{T}} . \end{aligned} \tag{C12}$$

The partial derivatives can be calculated from Eq. (18). Turning to a continuous description and using the normalization condition (C8) we find

$$\mathrm{Cov}(\hat{w}; z, z') = \frac{c}{\rho} \frac{\int \mathrm{d}z''\, p_z(z'') W_z(z, z'') W_z(z', z'')}{\int \mathrm{d}^2\theta'' \left|\gamma(\boldsymbol{\theta}'')\right|^2} \ . \tag{C13}$$

In the case $z = z'$, this equation has a simple interpretation. Let us call $N_W(z)$ the number of galaxies in the whole field for which $W_z\big(z, z^{(n)}\big)$ is significantly different from zero. Then the variance of $\hat{w}(z)$ is given simply by $c/\big[N_W(z)\big\langle|\gamma|^2\big\rangle\big]$, where $\big\langle|\gamma|^2\big\rangle$ is the mean value of the shear on the field. The covariance of $\hat{w}$ is in general proportional to $1/\big\langle|\gamma|^2\big\rangle$, and thus strong clusters should be preferred. However, as discussed before, for strong clusters the sheet invariance can generate serious problems in the determination of $w(z)$. This simple reasoning also clarifies the behaviour of $\mathrm{Cov}(\hat{w}; z, z')$ as a function of the weight $W_z(z, z')$ used. Since the expected variance of $\hat{w}(z)$ is proportional to $1/N_W(z)$, broad functions $W_z(z, z')$ should be preferred. However it is clear that the coherence length of $\hat{w}$, i.e. the maximum value of $|z - z'|$ that makes $\mathrm{Cov}(\hat{w}; z, z')$ significantly different from zero, is given by $N_W(z)$: this would suggest the use of a function W_z with small $N_W(z)$.

Eq. (C13) has been calculated assuming a generic shear map $\gamma(\boldsymbol{\theta})$. In practice, the shear used to calculate $\hat{w}(z)$ is the estimation $\hat{\gamma}(\boldsymbol{\theta})$, and thus $\gamma(\boldsymbol{\theta})$ in Eq. (C13) should be replaced by $\hat{\gamma}(\boldsymbol{\theta})$.

C.1.3. Role of the global scaling invariance

So far no assumption on $w(z)$ has been made. If we consider the expectation value of $\hat{\gamma}$, we see that the *assumed* cosmological weight enters through the quantity K. We have already observed that indeed this quantity is related to the global scaling invariance. In contrast to the expression for $\langle\hat{\gamma}\rangle$, the expected covariance of $\hat{\gamma}$, given by Eq. (C11), has a more complicated dependence on $w(z)$. When $K = 1$ the measured $\langle\hat{w}\rangle(z)$ is closest to the true $w_0(z)$ (see Eq. (C7)). From Eq. (C11) we see that the minimum of $\mathrm{Cov}(\hat{\gamma})$, under the constraint $K = 1$, is attained when $\int \mathrm{d}z'\, w(z') w_0(z')$ is maximum. It is then easy to show, using the Cauchy-Schwarz inequality, that this occurs when $w(z) = w_0(z)$.

The situation for the covariance of $\hat{w}$ is different. In fact, from Eq. (C13), it is clear that the constant K does not enter explicitly in the expression of this covariance. This property will play an important role in the statistical analysis of Appendix D.

In conclusion, the global scaling invariance, represented by the quantity K, has different effects on the various quantities. This quantity enters directly in the expressions of the expected values of $\hat{\gamma}$ and $\hat{w}$, while the expression for $\mathrm{Cov}(\hat{w})$ is not affected. However, the expected values of the shear and of the cosmological weight differ for an important characteristic. In fact, if the global scaling invariance could be broken, γ would be estimated also without the knowledge of $w(z)$ (see Eq. (C3)), while $w(z)$ cannot be calculated without the knowledge of γ. Therefore, the covariance of $\hat{\gamma}$, defined as $\big\langle\big(\hat{\gamma}(\boldsymbol{\theta}) - \langle\hat{\gamma}\rangle(\boldsymbol{\theta})\big)\big(\hat{\gamma}(\boldsymbol{\theta}') - \langle\hat{\gamma}\rangle(\boldsymbol{\theta}')\big)\big\rangle$, can be identified with the error $\big\langle\big(\hat{\gamma}(\boldsymbol{\theta}) - \gamma_0(\boldsymbol{\theta})\big)\big(\hat{\gamma}(\boldsymbol{\theta}') - \gamma_0(\boldsymbol{\theta}')\big)\big\rangle$ even if the cosmological weight used is not a good representation of w_0. The same, of course, is not true for w, since there is no relation between $\langle w\rangle$ and w_0, if the shear map used differs significantly from γ_0.

C.2. General case

Calculations for the general case are *exceedingly* difficult. If the lens is not too strong (say, $|g| < 0.5$) we might argue that a first approximation could be given by the results of the previous section. A posteriori, numerical simulations (described in the

main text) confirm the applicability of the weak lensing analysis to relatively strong lenses. On the other hand, if the lens is not weak and the sheet invariance cannot be broken, we have already shown that the method described here is difficult to apply.

Appendix D: extraction of cosmological information

We now have all the tools ready, in order to proceed from the estimation of $w(z)$ to the desired constraints on the cosmological parameters. In order to describe practically this function, we start by *discretizing* the problem in the redshift variable, which so far, for simplicity, has been kept continuous. We consider a grid of points $\{z_i\}$, with $i = 1, \ldots, N_z$. We then introduce the notation

$$w_i = w(z_i) \ , \tag{D1}$$

$$\langle \hat{w}_i \rangle = \langle \hat{w} \rangle (z_i) \ , \tag{D2}$$

$$Z_{ij} = \mathrm{Cov}(\hat{w}; z_i, z_j) \ , \tag{D3}$$

for the cosmological weight function, its expectation value, and its covariance on such a grid. At least for the weak lensing limit, the expression for $\langle \hat{w}_i \rangle$ and Z_{ij} can now be taken to be known (see Eqs. (C7) and (C13)). A similar discretization is performed in the $\boldsymbol{\theta}$-space. The least squares method for the extraction of the cosmological information focuses on the study of the *chi-square* function:

$$\chi^2(\xi) = \big(k\langle \hat{w}_i \rangle - \hat{w}_i\big) \big(Z^{-1}\big)_{ij} \big(k\langle \hat{w}_j \rangle - \hat{w}_j\big) \ , \tag{D4}$$

with $\xi = (\Omega, \Omega_\Lambda, k)$ a point in the parameter space Ξ. The ambiguity associated with the global scaling invariance is recognized and taken into account by means of the scale k which is treated as a free parameter in addition to the physical parameters Ω and Ω_Λ that we would like to constrain. Note that Ω and Ω_Λ enter in a complicated, non-linear manner, through the convolution of w_0 in the expression for $\langle \hat{w} \rangle$. The study of $\chi^2(\xi)$ can be addressed with three different goals.

D.1. Point estimation

Here one is interested in determining the most probable values of the cosmological parameters. These are the values $\hat{\xi}$ that minimize χ^2, obtained by solving the set of equations

$$\left. \frac{\partial \chi^2}{\partial \xi} \right|_{\hat{\xi}} = 0 \ . \tag{D5}$$

This could be completed with a determination of the related errors.

Here we should recall that the least squares estimation has the following properties (see Eadie et al. 1971): (i) If the expectation values $\langle \hat{w}_i \rangle$ have been determined correctly, then the estimation is *consistent*, i.e. it leads to the true cosmological parameters in the limit $N \to \infty$. (ii) If the measured weights $\hat{w}_i$ follow a Gaussian distribution, then the least squares method is equivalent to the maximum likelihood method. This occurs when the number of galaxies is sufficiently high ($N_W(z) \gtrsim 10$). (iii) If the mean $\langle \hat{w} \rangle (z)$ is a linear function of the parameters, or if a linear approximation can be used, the Gauss-Markov theorem states that the least squares method has minimum variance among the *unbiased* estimators that are *linear functions* of the observed quantities. This last property reassures us of the quality of the method used. Fortunately, at least for the scale parameter k the theorem holds.

D.2. Interval estimation

The interval estimation aims at identifying the relevant *confidence regions* in the parameter space Ξ, starting from a given *confidence level*, $CL < 1$. The region is usually determined by referring to the chi-square probability distribution, which depends on the number of degrees of freedom.

In the present case, given the values of the cosmological parameters, measurements of the cosmological weight will be realized (in the space of all possible measurements) with some probability distribution. Let us isolate in such a space a region with the following property: the probability that a set of measurements $\{\hat{w}_i\}$ be realized inside it is greater than a desired level, the confidence level CL. Suppose that a change of variables from $\{w_i\}$ to $\{v_i\}$ can be found such that the corresponding region in the new v-space does not depend on the cosmological parameters. Then, given one set of measurements $\{\hat{w}_i\}$, we may associate that region in v-space to the so-called confidence region in parameter space.

Our case requires additional discussion because one of the parameters, the scale k, is non-physical, and we are interested in defining confidence regions in the Ω-Ω_Λ plane. In order to do so, we might project the region found in the Ξ-space onto the plane of physical parameters. Since k can be ignored, an efficient approach is the following. We note that if we minimize χ^2 with respect to one parameter, the new quantity follows asymptotically ($N \to \infty$) a chi-square distribution with $N_z - 1$ degrees of freedom. Therefore, we may introduce the quantity

$$\ell_2(\Omega, \Omega_\Lambda) = \min_k \chi^2(\xi) - \chi^2(\hat{\xi}) \ , \tag{D6}$$

which is expected to follow a chi-square distribution with two degrees of freedom. With this device, the confidence regions can be drawn in a straightforward way, independently of the number N_z of points in the redshift grid. For finite values of N, ℓ_2 is not required to follow strictly a chi-square distribution with two degrees of freedom; however, ℓ_2 is always a reasonable statistic.

The method described above turns out to be just an application of the well-known "likelihood ratio" method to our problem (with the global scaling invariance taken into account). In fact, it can be shown that the quantity ℓ_2 can be expressed as

$$\ell_2(\Omega, \Omega_\Lambda) \ = \ 2 \sum_{n=1}^{N} \Big[\ln \mathcal{L}\big(\epsilon^{(n)} \ \big| \ \hat{\Omega}, \hat{\Omega}_\Lambda, \hat{k}, \hat{\gamma}(\boldsymbol{\theta}^{(n)})\big) - \ln \mathcal{L}\big(\epsilon^{(n)} \ \big| \ \Omega, \Omega_\Lambda, \hat{k}, \hat{\gamma}(\boldsymbol{\theta}^{(n)})\big) \Big] \ . \tag{D7}$$

In this expression $\mathcal{L}$ is the "likelihood" for a single galaxy (see Eadie et al. 1971), i.e. the probability of observing a galaxy with ellipticity $\epsilon^{(n)}$ when the shear is $\gamma(\boldsymbol{\theta})$ and when the "cosmological" parameters are Ω, Ω_Λ, and k. Then, using the central

limit theorem and the results (C7) and (C13) for the mean and the covariance of the cosmological weight, the relation between Eq. (D6) and (D7) follows.

The quantity ℓ_2 will prove to be useful also as a test of hypotheses, as explained below.

D.3. Test of hypotheses

The third analysis that can be performed on the measured cosmological weight is the test of hypotheses. In this case a given hypothesis h_0, called "null hypothesis," is tested against an alternative hypothesis h_1. A test is a method to choose between h_0 and h_1 from a given set of observations. Hence it can be thought as a region in the space of the observed quantities: if the point representing the observations lies inside this area, the null hypothesis is true, otherwise it is false.

All hypotheses that we may be interested in testing would actually be *composite* hypotheses, because of the presence of the scale parameter k. Let Ξ_0 be the subset of Ξ for which the null hypothesis is true (for example, $\Omega + \Omega_\Lambda = 1$, with k arbitrary). Then the alternative hypothesis holds on the set $\Xi \setminus \Xi_0$. The likelihood ratio is defined as

$$l = \frac{\max\limits_{\xi\in\Xi_0} \mathcal{L}\big(\epsilon^{(n)} \mid \xi\big)}{\max\limits_{\xi\in\Xi} \mathcal{L}\big(\epsilon^{(n)} \mid \xi\big)} \; . \tag{D8}$$

Clearly $0 \le l \le 1$. Then, the likelihood ratio test is given by the following rule: if $l < l_0$ then choose h_0, otherwise choose h_1. The limiting value l_0 has to be chosen so that the probability of "loss error" (i.e., the rejection of the null hypothesis when in reality h_0 is true) is small, and the threshold value may be set, for example, at 5%. Such a test is found empirically to produce useful and significant results.

If we want to test a hypothesis h_0 fixing separately the values of Ω and Ω_Λ (so that Ξ_0 reduces to a straight line), by combining the discussion of Eq. (D7) with that of Eq. (D8) we see that we can express ℓ_2 in terms of χ^2 as

$$\ell_2 = -2\ln l = \min_{\xi\in\Xi_0} \chi^2(\xi) - \min_{\xi\in\Xi} \chi^2(\xi) \; . \tag{D9}$$

Thus it can be shown that, if the h_0 hypothesis is true, the quantity $(-2\ln l)$ follows (asymptotically) a chi-square distribution with two degrees of freedom.

For different types of h_0 the quantity $(-2\ln l)$ follows (asymptotically) a chi-square distribution with degrees of freedom equal to the number of parameters fixed by h_0.

At this point, the "level of acceptance" can be obtained from the cumulative chi-square distribution for the relevant number of degrees of freedom. In particular, if we want to test the Einstein-de Sitter universe ($\Omega = 1$, $\Omega_\Lambda = 0$) with 5% significance, we use the statistic

$$\ell_2 = \min_k \chi^2(1, 0, k) - \chi^2(\hat{\xi}) \; . \tag{D10}$$

The universe will be considered Einstein-de Sitter if $\ell_2 < 5.991$. If, instead, we want to test the flat hypothesis ($\Omega + \Omega_\Lambda = 1$) with significance 5%, we use the statistic

$$\ell_1 = \min_{\Omega,k} \chi^2(\Omega, 1-\Omega, k) - \chi^2(\hat{\xi}) \; . \tag{D11}$$

The universe will be considered to be flat if $\ell_1 < 3.841$.

As noted earlier, when the asymptotic ($N \to \infty$) limit is not justified, one should resort to Monte Carlo simulations in order to set the appropriate "level of acceptance."

References

Baum W.A., 1962, In: McVittie G.C. (ed.) IAU Symp. 15, Problems of extra-galactic research. 390

Bartelmann M., Narayan R., 1995, ApJ 451, 60

Brainerd T., Blandford R., Smail I., 1996, ApJ 466, 623

Broadhurst T.J., Taylor A.N., Peacock J.A., 1995, ApJ 438, 49

Clowe D., Luppino G.A., Kaiser N., Henry J.P., Gioia I.M., 1998, ApJ 497, L61

Driver S.P., Fernández-Soto A., Couch W.J., et al., 1998, ApJ 496, L93

Eadie W.T., Drijard R., James F.E., Roos M., Sadoulet B., 1971, Statistical methods in experimental physics. North-Holland, Oxford, UK

Hoekstra H., Franx M., Kuijken K., Squires G., 1998, ApJ 504, 636

Hogg D.W.,et al., 1998, AJ 115, 4, 1418

Kaiser N., 1995, ApJ 493, L1

Kaiser N., Squires G., 1993, ApJ 404, 441

Kaiser N., Squires G., Broadhurst T.J., 1995, ApJ 449, 460

Kayser R., Helbig P., Schramm T., 1997, A&A 318, 680

Lanzetta K.M., Yahil A., Fernández-Soto A., 1996, Nat 381, 759

Lombardi M., 1996, Tesi di Laurea, Università di Pisa

Lombardi M., Bertin G., 1998a, A&A 330, 791 (Paper I)

Lombardi M., Bertin G., 1998b, A&A 335, 1 (Paper II)

Luppino G.A., Kaiser N., 1997, ApJ 475, 20

Peebles P.J.E., 1993, Principles of Physical Cosmology. Princeton University Press, Princeton

Press W.H., Teukolsky S.A., Vetterling W.T., Flannery B.P., 1992, Numerical Recipes in C. Cambridge University Press, Cambridge

Schneider P., Elhers J., Falco E.E., 1992, Gravitational Lenses. Springer-Verlag, Berlin

Schneider P., Seitz C., 1995, A&A 294, 411

Seitz C., Schneider P., 1995, A&A 297, 287

Seitz S., Schneider P., 1996, A&A 305, 383

Seitz C., Schneider P., 1997, A&A 318, 687

Stiavelli M., Stockman P., Burg R., 1997, Next Generation Space Telescope – design reference mission. ST-ECF Newsletter 24, 4

Tyson J.A., Valdes F., Jarvis J.F., Mills A.P., 1984, ApJ 281, L59